



HAL
open science

A New Glideslope Guidance Algorithm for Minimum-Fuel Fixed-Time Elliptic Rendezvous Using Semidefinite Programming

Yassine Ariba, Denis Arzelier, Laura Sofia Urbina

► **To cite this version:**

Yassine Ariba, Denis Arzelier, Laura Sofia Urbina. A New Glideslope Guidance Algorithm for Minimum-Fuel Fixed-Time Elliptic Rendezvous Using Semidefinite Programming. IFAC World Congress 2017, Jul 2017, Toulouse, France. pp.7235 - 7240, 10.1016/j.ifacol.2017.08.1369 . hal-01887913

HAL Id: hal-01887913

<https://laas.hal.science/hal-01887913>

Submitted on 11 Oct 2018

HAL is a multi-disciplinary open access archive for the deposit and dissemination of scientific research documents, whether they are published or not. The documents may come from teaching and research institutions in France or abroad, or from public or private research centers.

L'archive ouverte pluridisciplinaire **HAL**, est destinée au dépôt et à la diffusion de documents scientifiques de niveau recherche, publiés ou non, émanant des établissements d'enseignement et de recherche français ou étrangers, des laboratoires publics ou privés.

A New Glideslope Guidance Algorithm for Minimum-Fuel Fixed-Time Elliptic Rendezvous Using Semidefinite Programming

Yassine Ariba ^{*,**}, Denis Arzelier ^{**}, Laura Sofia Urbina ^{**},

^{*} ICAM, 75 avenue de Grande Bretagne, 31300 Toulouse, France
(email: yassine.ariba@icam.fr)

^{**} CNRS, LAAS, 7 avenue du colonel Roche, F-31400 Toulouse, France and Univ de Toulouse, LAAS, F-31400 Toulouse, France
(e-mails: yariba@laas.fr, arzelier@laas.fr, lsurbina@laas.fr).

Abstract: This paper presents a new minimum-fuel glideslope guidance algorithm for approaching a target evolving on an elliptic orbit. In addition to the usual rectilinear profile to follow as in Hablani's seminal paper, two new features are requested for the new algorithm. The first one imposes bounds on the guidance error inherent to chemical propulsion glideslope guidance, such that the chaser's trajectory does not escape from an admissible domain. The second one minimizes the consumption during rendezvous. Indeed, unlike the classical glideslope algorithm for which there is no direct control on the fuel consumption, additional degrees of freedom and relevant decision variables may be identified. By combining a useful parametrization of the Tschauner-Hempel relative equations of motion and results from polynomial optimization, a semidefinite formulation of the constraints on the maximal guidance error is obtained. For a fixed-time glideslope rendezvous with a pre-assigned number of maneuvers, a fuel-optimal solution with a bounded guidance error is obtained by solving a semidefinite programming problem. Two numerical examples illustrate the usefulness of the method compared to the classical ones when the approach corridor has to verify stringent geometrical restrictions such as line-of-sight constraints.

Keywords: Glideslope approach, impulsive control, elliptic rendezvous, Tschauner-Hempel equations, semidefinite programming

1. INTRODUCTION

Rendezvous (RDV) between two spacecraft (a target and a chaser) has been one of the most salient operational technology since its first manual achievement in the sixties between a Gemini vehicle and an unmanned target vehicle. Recently, an increasing demand is witnessed to perform autonomous rendezvous, proximity or On-Orbit Servicing operations between an active chaser spacecraft and a passive target spacecraft. Autonomy means that appropriate RDV guidance schemes should combine the simplicity of onboard implementation and a low level of fuel consumption. The objective of the closing phase is to steer the chaser from several kilometers to few hundreds of meters near the orbital target applying short high thrust pulses approximated as impulsive maneuvers. This idealization of the real actuation may greatly simplify the design of efficient guidance schemes for close range rendezvous operations (Fehse (2003)). The impulsive approximation consists of instantaneous velocity increments which are applied to the actuated spacecraft whereas its position remains unchanged.

This paper focuses on the fixed-time linearized minimum-fuel impulsive closing phase rendezvous problem. Depending on various operational and safety constraints, various closing phase strategies may be envisioned and proposed to realize the proximal rendezvous: V-bar (curvilinear orbit direction as a straight line) and R-bar (direction of the center of attraction) are very classical approaches while looping trajectory or natural drift orbit to R-bar approach are interesting variations as described by Fehse (2003).

Observability (line-of-sight constraints), safety reasons and fuel budget are the main incentives to make a choice among all possible approaches. One simple and general scheme complying to safety restrictions is known as the glideslope approach. This trajectory is a straight path in any direction connecting the current location of the chaser to its final destination. The glideslope approach has been first defined in the past for rendezvous and proximity operations involving the space shuttle (Pearson (1989)). This preliminary study has been extended and generalized later for any direction in space and circular reference orbit in Hablani et al. (2002), Wang et al. (2007) and for elliptic reference orbit in Okasha and Newman (2011). Indeed, the results presented in Hablani et al. (2002) are well-known and define the so-called classical glideslope algorithm.

Our goal is to extend a previous work from Ariba et al. (2016) where the classical glideslope algorithm of Hablani was revisited in specific cases (V-bar and R-bar approaches) to the general setup and for an elliptic reference orbit. The objective is to identify a new formulation of the problem including useful degrees of freedom that allows to minimize the fuel consumption and helps to enclose the resulting trajectory segments between two successive maneuvers, usually referred to as hopping, in a user-defined approach corridor. Indeed, combining a suitable parametrization of the Tschauner-Hempel relative equations of motion and results from polynomial optimization, a semidefinite programming problem is obtained and gives a minimum-fuel solution to the glideslope guidance problem while controlling the guidance error. The proposed algorithm is compared to the classical glideslope algo-

rithm on two numerical examples, illustrating the interest of this new approach in terms of consumption reduction and admissibility of the trajectory in a visibility corridor.

Notations: $O_{p \times m}$ and I_m denote respectively the null matrix of dimensions $p \times m$, the identity matrix of dimension m . In order to simplify the notation, the transition matrix $\Phi(t_{k+1}, t_k)$ will be denoted $\Phi^{[k]}$. For a symmetric real matrix $S \in \mathbb{R}^{n \times n}$, the notation $S \preceq 0$ ($S \succeq 0$) stands for the negative (positive) semi-definiteness of S .

2. CLASSICAL GLIDESLOPE APPROACH FOR RENDEZVOUS

2.1 Relative motion dynamics

The close range phase of the spacecraft rendezvous mission is characterized by the use of relative navigation since the separation between spacecraft is sufficiently small (Fehse (2003)). When relative navigation information is available to the chaser, the relative motion of the chaser is expressed in the Local-Vertical-Local-Horizontal (LVLH) frame. The origin of the coordinate frame is located at the center of mass of the leader and the space is spanned by $(\mathbf{x}, \mathbf{y}, \mathbf{z})$ where the \mathbf{z} axis is in the radial direction (R-bar) oriented towards the center of the Earth, the \mathbf{y} axis is perpendicular to the leader orbital plane and pointing in the opposite direction of the angular momentum (H-bar) while the \mathbf{x} axis completes the right-hand triad $\mathbf{x} = \mathbf{y} \times \mathbf{z}$ (V-bar), see Figure 1. The vector \mathbf{r} defines the relative position of the chaser with respect to the target.

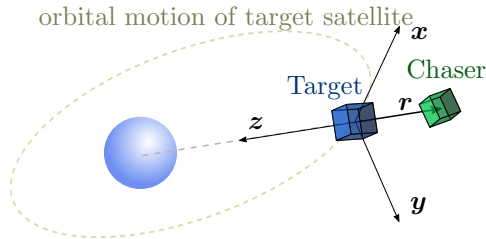


Fig. 1. LVLH frame for spacecraft rendezvous.

Under Keplerian assumptions (no orbital perturbations are considered) and an elliptic reference orbit, the equations of motion for the relative motion in the LVLH frame may be linearized for close separation between the leader and the follower (Alfriend et al., 2010, Chapter 5, Section 5.6.1).

$$\dot{X}(t) = A_0(t)X(t) + \begin{bmatrix} O_{3 \times 3} \\ I_3 \end{bmatrix} \frac{f(t)}{m_F} \quad (1)$$

where state $X = (x, y, z, dx/dt, dy/dt, dz/dt)^T$ represents positions and velocities in the three fundamental axes of the LVLH frame, $f(t) = [f_x(t) f_y(t) f_z(t)]^T$ is the thrust vector, m_F is the mass of the follower and the dynamic matrix $A_0(t)$ is a periodic matrix of time t given by :

$$A_0(t) = \begin{bmatrix} 0 & 0 & 0 & 1 & 0 & 0 \\ 0 & 0 & 0 & 0 & 1 & 0 \\ 0 & 0 & 0 & 0 & 0 & 1 \\ a_1(t) & 0 & \ddot{\nu} & 0 & 0 & 2\dot{\nu} \\ 0 & a_2(t) & 0 & 0 & 0 & 0 \\ -\ddot{\nu} & 0 & a_3(t) & -2\dot{\nu} & 0 & 0 \end{bmatrix}, \quad (2)$$

and

$$\begin{aligned} a_1(t) &= \dot{\nu}^2 - k^4 \eta(\nu)^3, \\ a_2(t) &= -k^4 \eta(\nu)^3, \\ a_3(t) &= \dot{\nu}^2 + 2k^4 \eta(\nu)^3. \end{aligned}$$

Note that:

$$\frac{d\nu}{dt} = \frac{n}{(1 - e^2)^{3/2}} \underbrace{(1 + e \cos \nu)^2}_{\eta(\nu)} =: k^2 \eta(\nu)^2, \quad (3)$$

and $n = \sqrt{\frac{\mu}{a^3}} = 2\pi/T$ is the mean motion of the leader orbit and μ is the standard gravitational parameter. It is assumed that only the chaser is active and has actuators using 6 un gimbaled identical chemical thrusters. The use of chemical propulsion leads to idealize possible thrusts as impulsive maneuvers providing instantaneous velocity jumps in the three axes while the relative position remains unchanged during firing. The impulsive control input is thus defined as:

$$\Delta v(t_k) := \Delta v_k := \int_{t_k^-}^{t_k^+} \frac{1}{m_F} \begin{bmatrix} f_x(t) \\ f_y(t) \\ f_z(t) \end{bmatrix} dt, \quad (4)$$

where t_k is a generic firing time and Δv_k represents the applied impulsive thrust. In order to compute the transition matrix $\Phi(t, t_0)$ for the linearized equations (1), classical derivations dating back to the seminal publications of Lawden (Lawden, 1963, Chapter 5) and Tschauner-Hempel (Tschauner (1967)) consists in applying a change of independent variable from time t to true anomaly ν and a simplifying coordinate change leading to $\tilde{X}(\nu) = T(\nu)X(t)$ with

$$T(\nu) := \begin{bmatrix} \eta(\nu)I_3 & O_{3 \times 3} \\ \eta(\nu)'I_3 & \frac{1}{k^2 \eta(\nu)}I_3 \end{bmatrix}. \quad (5)$$

The obtained simplified autonomous state space representation is expressed as $\tilde{X}'(\nu) = \tilde{A}(\nu)\tilde{X}(\nu)$ where

$$\tilde{A}(\nu) = \begin{bmatrix} 0 & 0 & 0 & 1 & 0 & 0 \\ 0 & 0 & 0 & 0 & 1 & 0 \\ 0 & 0 & 0 & 0 & 0 & 1 \\ 0 & 0 & 0 & 0 & 0 & 2 \\ 0 & -1 & 0 & 0 & 0 & 0 \\ 0 & 0 & \frac{3}{\eta(\nu)} & -2 & 0 & 0 \end{bmatrix}. \quad (6)$$

Although this state-space equation is linear time-varying, $\tilde{A}(\nu)$ is simple enough to allow for the derivation of the autonomous solution via the computation of a fundamental matrix $\tilde{\varphi}_{\nu_0}(\nu)$ and a transition matrix $\tilde{\Phi}(\nu, \nu_0)$. Based on a particular fundamental solution, the so-called Yamanaka-Ankersen form of the transition matrix, has been proposed in the reference Yamanaka and Ankersen (2002). This form is particularly appealing for computation purposes and therefore the transition matrix $\Phi(t, t_0)$ may be considered as readily computable by:

$$\Phi(t, t_0) = T(\nu)^{-1} \tilde{\varphi}_{\nu_0}(\nu) \tilde{\varphi}_{\nu_0}(\nu_0)^{-1} T(\nu_0). \quad (7)$$

Thus, a controlled trajectory composed of $N + 1$ impulses is described by the following equation:

$$X(t) = \Phi(t, t_0)X(t_0) + \sum_{k=0}^N \Phi(t, t_k)B\Delta v_k, \quad (8)$$

where $t_1 < t_2 < \dots < t_N \leq t$ and Δv_k denotes the impulsive control applied at t_k . $B = [O_{3 \times 3} \ I_3]^T$ is the input matrix. Hereafter, the following notation describing the free motion with a block partitioned transition matrix is adopted:

$$X(t) = \begin{bmatrix} \mathbf{r}(t) \\ \mathbf{v}(t) \end{bmatrix} = \begin{bmatrix} \Phi_{rr}(t, t_0) & \Phi_{rv}(t, t_0) \\ \Phi_{vr}(t, t_0) & \Phi_{vv}(t, t_0) \end{bmatrix} \begin{bmatrix} \mathbf{r}_0 \\ \mathbf{v}_0 \end{bmatrix}. \quad (9)$$

2.2 Hablani's classical glideslope approach

When considering design of impulsive maneuvers for a glideslope rendezvous, the most cited reference is the paper by Hablani et al. (2002) in which the so called classical inbound and outbound glideslope approaches for circular reference are presented in a general setup. This guidance trajectory is characterized by a straight line and its associated vector $\boldsymbol{\rho}(\nu) = \mathbf{r}_c(\nu) - \mathbf{r}_T$, defining the commanded path as illustrated by the Figure 2. Defining $\boldsymbol{\rho}_0 = \mathbf{r}_0 - \mathbf{r}_T$, the unit vector \mathbf{u} gives the direction of the straight path:

$$\mathbf{u} = \begin{bmatrix} \frac{x_T - x_0}{\|\boldsymbol{\rho}_0\|} & \frac{y_T - y_0}{\|\boldsymbol{\rho}_0\|} & \frac{z_T - z_0}{\|\boldsymbol{\rho}_0\|} \end{bmatrix}^T.$$

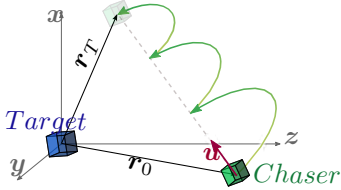


Fig. 2. Glideslope approach.

The chaser has to reach \mathbf{r}_T from \mathbf{r}_0 following a specific commanded profile:

$$\boldsymbol{\rho}(t) = \rho_0 e^{\frac{(\dot{\rho}_0 - \dot{\rho}_T)t}{\omega\rho_0}} + \frac{\dot{\rho}_T \rho_0}{\dot{\rho}_0 - \dot{\rho}_T} \begin{pmatrix} e^{\frac{(\dot{\rho}_0 - \dot{\rho}_T)t}{\omega\rho_0}} - 1 \\ \end{pmatrix},$$

where $\dot{\rho}_0 < 0$, $\dot{\rho}_T < 0$ are respectively the initial and final approach velocities and $\rho_0 = \|\boldsymbol{\rho}_0\|$ is the initial distance to go. These quantities are specified by the designer and inputs for the classical algorithm. Note that $\dot{\rho}_0 > \dot{\rho}_T$ and that $\rho_T = 0$ by definition of the trajectory. For a given set of these parameters, the basic principle of the classical algorithm is then to analytically compute a fixed number of impulses equally spaced in time over the transfer duration T . Each computed incremental velocity at \mathbf{r}_k is obtained as $\Delta \mathbf{v}_k = \mathbf{v}_{k+} - \mathbf{v}_{k-}$ where \mathbf{v}_{k+} is the departure velocity needed to go from \mathbf{r}_k to \mathbf{r}_{k+1} and \mathbf{v}_{k-} is the arrival velocity at \mathbf{r}_k . Both quantities are simply obtained by solving the autonomous Hill-Clohessy-Wiltshire equations (Clohessy and Wiltshire (1960)) at each step k .

The classical glideslope algorithm is straightforward and rapid to implement but suffers from key shortcomings. First, it is limited to circular reference orbits. In addition, it is important to mention that the actual trajectory of the chaser will not be strictly along the commanded straight line path but will exhibit humps between the N points where an impulsive maneuver is performed and located on the commanded path (cf. Figure 2). These humps come from the natural relative motion of the chaser driven by the Hill-Clohessy-Wiltshire equations and cannot be directly controlled by the algorithm. Moreover, there is no degree of freedom to control the transfer time and the consumption. Indeed, the transfer time T is not fixed *a priori* but deduced from the initial and final commanded velocities ($\dot{\rho}_0, \dot{\rho}_T$) and from the initial distance to go ρ_0 :

$$T = \frac{\rho_0}{\dot{\rho}_0 - \dot{\rho}_T} \ln \left[\frac{\dot{\rho}_T}{\dot{\rho}_0} \right].$$

The consumption itself is computed *a posteriori* from the velocity increments without any possibility to optimize it for given end conditions of the rendezvous. The objective of the present paper is therefore to propose a new optimization algorithm for the general glideslope framework

and extend the results to elliptic reference orbits, taking these two important features into account:

- Minimize the fuel-consumption for a given set of initial and final rendezvous conditions and an *a priori* fixed time of transfer;
- Control the maximum guidance error by defining constraints on the humps profile.

3. MINIMUM-FUEL GLIDESLOPE APPROACH WITH CONTROLLED HUMPS VIA SEMIDEFINITE PROGRAMMING

The main result of the paper is now presented. It mainly consists in deriving a numerically tractable expression for different constraints on the chaser trajectory while identifying suitable decision variables. This modeling work and the introduction of degrees of freedom lead to the formulation of an optimization problem allowing to minimize the fuel consumption during the glideslope transfer.

3.1 Glideslope line tracking

In order to perform the transfer from \mathbf{r}_0 to \mathbf{r}_T in a given duration T , the number of thruster firings is fixed and equal to N . Any two successive impulsive maneuvers are separated by $\Delta t = T/N$ and impulsive thrusts are applied at dates $t_k = k\Delta t$, $k = 0, 1, \dots, N-1$. The following notation will be used in the rest of the paper.

$$\mathbf{r}(t_k) = \mathbf{r}_k, \quad \boldsymbol{\rho}(t_k) = \boldsymbol{\rho}_k, \quad \mathbf{v}(t_k) = \mathbf{v}_k.$$

Throughout the transfer, the spacecraft must follow the commanded path. After each maneuver, the chaser must be back on the glideslope line. The initial \mathbf{r}_0 and final $\mathbf{r}_N = \mathbf{r}_T$ positions are fixed by specifications. Intermediate positions are set free and are parameterized as

$$\mathbf{r}_k = \mathbf{r}_0 + \rho_k \mathbf{u}, \quad k = 1, \dots, N-1. \quad (10)$$

The scalars ρ_k are free and denote the travelled distance from \mathbf{r}_0 to \mathbf{r}_k . Note that $\rho_0 = 0$ and $\rho_N = \|\mathbf{r}_T - \mathbf{r}_0\|$. A set of N equations of the form:

$$\mathbf{r}_{k+1} = \Phi_{rr}^{[k]} \mathbf{r}_k + \Phi_{rv}^{[k]} \mathbf{v}_{k+}, \quad k = 0, \dots, N-1, \quad (11)$$

with the position vectors $\mathbf{r}_{k+1} / \mathbf{r}_k$ as defined above, defines the relative dynamics of the chaser after the impulsive actuation at t_k . \mathbf{v}_{k+} is the velocity vector right after the impulse is applied. Combining Equations (10) and (11) enforces the requirement for the chaser to come back on the path after each maneuver period leading to the set of equations:

$$\begin{aligned} \rho_{k+1} \mathbf{u} - \rho_k \Phi_{rr}^{[k]} \mathbf{u} - \Phi_{rv}^{[k]} \mathbf{v}_{k+} &= (\Phi_{rr}^{[k]} - I_3) \mathbf{r}_0, \\ \rho_1 \mathbf{u} - \Phi_{rv}^{[0]} \mathbf{v}_{0+} &= (\Phi_{rr}^{[0]} - I_3) \mathbf{r}_0, \end{aligned} \quad (12)$$

for $k = \{1, \dots, N-1\}$. Because the reference orbit is considered to be elliptic, the transition matrix is not constant all over the orbit and needs to be updated for each maneuver. Since time intervals for impulse control are input data, all transition matrices $\Phi^{[k]}$ can be computed *a priori*. The decision variables in (12) are composed by the sequence of scalar variables ρ_k for $k = 1, \dots, N-1$ and by the sequence of vectors \mathbf{v}_{k+} for $k = 0, 1, \dots, N-1$. The sequence of impulses is deduced afterwards, computing the difference between the design variable \mathbf{v}_{k+} and the velocity vector \mathbf{v}_{k-} resulting from the previous maneuver and from the relative dynamics of the chaser:

$$\mathbf{v}_{k+1-} = \Phi_{vr}^{[k]} \mathbf{r}_k + \Phi_{vv}^{[k]} \mathbf{v}_{k+}, \quad k = 0, 1, \dots, N-1.$$

Therefore, we have $\Delta \mathbf{v}_k = \mathbf{v}_{k+} - \mathbf{v}_{k-}$.

3.2 Final velocity constraint

Since a last impulse is needed to control the final velocity of the spacecraft, an additional equality constraint is defined. This $(N + 1)^{th}$ impulse maneuver is given by:

$$\Delta \mathbf{v}_N = \mathbf{v}_{N+} - \Phi_{vr}^{[N-1]} \mathbf{r}_{N-1} - \Phi_{vv}^{[N-1]} \mathbf{v}_{N-1+}.$$

Setting the vector $\mathbf{v}_{N+} = \mathbf{v}_T$ as the desired final velocity and $\Delta \mathbf{v}_N$ being a free variable, an extra equality constraint is appended:

$$\mathbf{v}_T - \Phi_{vr}^{[N-1]} \mathbf{r}_0 = \Phi_{vr}^{[N-1]} \mathbf{u}_{\rho_{N-1}} + \Phi_{vv}^{[N-1]} \mathbf{v}_{N-1+} + \Delta \mathbf{v}_N. \quad (13)$$

3.3 Constraints on guidance error

The aim of this subsection is to give a numerically tractable formulation of the continuous constraints imposed on the spacecraft relative trajectory in order to bound the guidance error inherent to the impulsive glideslope approach. In the spirit of the method developed in Deaconu et al. (2015), the idea is to look for an equivalent finite description of the admissible relative trajectories using various tools from algebraic geometry and in particular, properties of non-negative polynomials provided in Nesterov (2000).

First, a set of linear constraints on the chaser's relative trajectory is defined, for each maneuver, by:

$$A_k \mathbf{r}(t) \leq b_k, \quad \forall t \in [t_k, t_{k+1}], \quad \forall k = \{0, \dots, N-1\}. \quad (14)$$

The interval $[t_k, t_{k+1}]$ corresponds to the maneuver period, from the $(k + 1)^{th}$ impulse to the instant when the spacecraft is back on the glideslope line. $A_k \in \mathbb{R}^{n_c \times 3}$ is a constant matrix and $b_k \in \mathbb{R}^{n_c}$ is a constant vector. These matrices are built from input specifications related to the maximal allowable excursion. n_c denotes the number of scalar inequalities, each of which defines a plane bounding the trajectory. For instance, let us define vectors u_1 and u_2 as an orthonormal basis for the null space of \mathbf{u}^T . By choosing

$$A_0 = \begin{bmatrix} u_1^T \\ -u_1^T \\ u_2^T \\ -u_2^T \end{bmatrix} \quad \text{and} \quad b_0 = \begin{bmatrix} u_1^T (r_0 + \delta_1 u_1) \\ -u_1^T (r_0 - \delta_1 u_1) \\ u_2^T (r_0 + \delta_2 u_2) \\ -u_2^T (r_0 - \delta_2 u_2) \end{bmatrix}, \quad (15)$$

we define a rectangular corridor with four planes parallel to the glideslope direction. Parameters δ_1 and δ_2 specify the distance from the glideslope line to each pair of planes. Then, in this case, $n_c = 4$ and the matrix $A_k = A_0$ is identical $\forall k = \{0, \dots, N-1\}$. Vector b_k changes at each maneuver according to the different distance specifications $\{\delta_{1k}, \delta_{2k}\}$. Let us apply the change of variable (5) to the general constraint (14):

$$A_k \tilde{\mathbf{r}}(\nu) \leq \eta(\nu) b_k, \quad \forall \nu \in [\nu_k, \nu_{k+1}], \quad \forall k = \{0, \dots, N-1\}. \quad (16)$$

In Deaconu et al. (2015), the autonomous relative trajectory is parameterized as follows:

$$\begin{cases} \tilde{x}(\nu) = (2 + e \cos \nu)(d_1 \sin \nu - d_2 \cos \nu) + d_3 \\ \quad + 3d_4 J(\nu, \nu_0)(1 + e \cos \nu)^2, \\ \tilde{y}(\nu) = d_5 \cos \nu + d_6 \sin \nu, \\ \tilde{z}(\nu) = (1 + e \cos \nu)(d_2 \sin \nu + d_1 \cos \nu) \\ \quad - 3e d_4 J(\nu, \nu_0) \sin \nu (1 + e \cos \nu) + 2d_4, \end{cases}$$

for $\nu \in [\nu_0, \nu_f]$, where the parameters d_i depend linearly on the initial state at time ν_k . The integral term $J(\nu, \nu_0)$ is given by

$$J(\nu, \nu_0) = \int_{\nu_0}^{\nu} \frac{1}{\eta(u)^2} du = \frac{n}{(1 - e^2)^{3/2}} (t - t_0).$$

We are now in a position to apply the following change of variable in order to transform the trigonometrical functions into rational functions

$$w = \tan \frac{\nu}{2}, \quad \cos \nu = \frac{1 - w^2}{1 + w^2}, \quad \sin \nu = \frac{2w}{1 + w^2}. \quad (17)$$

The propagation of the spacecraft relative motion can then be expressed as a function of w :

$$\begin{cases} \tilde{x}(w) = \frac{1}{(1 + w^2)^2} [P_x(w) + 3d_4 P_{J_x}(w) J(w)], \\ \tilde{y}(w) = \frac{1}{(1 + w^2)} P_y(w), \\ \tilde{z}(w) = \frac{1}{(1 + w^2)^2} [P_z(w) + 2d_4 P_{J_z}(w) J(w)] \end{cases}$$

for $w \in [w_0, w_f]$. All P_* functions are polynomials whose coefficients depend linearly on the initial state at time w_0 , that is ν_k . Definitions and detailed calculations are given in Ariba et al. (2017). Only the term with $J(w)$ is non-rational and requires to be dealt with. To this end, a polynomial approximation is derived to bound J over $w \in [w_0, w_f]$:

$$J(w) = \Theta_r(w) + \varepsilon(w) \Rightarrow \underbrace{\Theta_r(w)}_{\Theta_l(w)} - \bar{\varepsilon} \leq J(w) \leq \underbrace{\Theta_r(w)}_{\Theta_u(w)} + \bar{\varepsilon}$$

where $\Theta_r(w)$ is a polynomial of degree r and $\bar{\varepsilon}$ the maximum error due to the approximation. The linear constraints (16) are transformed by the change of variables (17) into:

$$A_k \tilde{\mathbf{r}}(w) \leq \left(\frac{1 + e + (1 - e)w^2}{1 + w^2} \right) b_k,$$

$$\forall w \in [w_k, w_{k+1}], \quad \forall k = \{0, \dots, N-1\},$$

with $w_k = \tan(\nu_k/2)$. Replacing the function $J(w)$ by the two extreme bounding polynomials Θ_l and Θ_u , each row i of the above constraint is translated into two inequalities:

$$\begin{cases} \Gamma_{il}^k(w) \geq 0, \\ \Gamma_{iu}^k(w) \geq 0. \end{cases}$$

Γ_{il}^k and Γ_{iu}^k are two polynomials whose coefficients are linear w.r.t. the initial state at time w_k (see (Ariba et al., 2017)). This pair of inequalities must be repeated for each constraint i (i.e. rows of A_k) and for each maneuver k . The properties of non negative polynomials and representation theorems of cones of non negative polynomials given in Nesterov (2000) allow us to translate these inequalities defined on an infinite interval into a semi-definite programming problem:

$$\begin{cases} \exists Y_{1il}^k, Y_{2il}^k \succeq 0 \quad \text{s.t.} \quad \gamma_{il}^k = \Lambda^*(Y_{1il}^k, Y_{2il}^k), \\ \exists Y_{1iu}^k, Y_{2iu}^k \succeq 0 \quad \text{s.t.} \quad \gamma_{iu}^k = \Lambda^*(Y_{1iu}^k, Y_{2iu}^k), \end{cases} \quad (18)$$

for $i = \{1, \dots, n_c\}$, for $k = \{0, \dots, N-1\}$. Γ_{il}^k and Γ_{iu}^k are represented by their vector of coefficients γ_{il}^k and γ_{iu}^k , respectively. The exact definition of the linear operator Λ^* is omitted here for the sake of conciseness but it may be obtained in the appendix of the reference Deaconu et al. (2015).

3.4 Definition of the Cost function

The main objective of the proposed approach is to minimize the fuel consumption during the transfer. As 6 ungimbaled identical chemical thrusters are used, the cost function may be naturally defined as the 1-norm of the $N + 1$ impulsive thrusts:

$$C(N) = \sum_{k=0}^N \|\Delta \mathbf{v}_k\|_1, \quad (19)$$

with $\Delta \mathbf{v}_k = \mathbf{v}_{k+} - \mathbf{v}_{k-}$. The formulation (19) is transformed in order to express the above criterion with respect to the decision variables \mathbf{v}_{k+} , $k = 0, \dots, N-1$, ρ_k , $k = 1, \dots, N-1$ and Δv_N :

$$C(N) = \|\mathbf{v}_{0+} - \mathbf{v}_{0-}\|_1 + \|\Delta \mathbf{v}_N\|_1 + \sum_{k=1}^{N-1} \|\mathbf{v}_{k+} - \Phi_{vr}^{[k-1]}(r_0 + \rho_{k-1}u) - \Phi_{vv}^{[k-1]}\mathbf{v}_{k-1+}\|_1,$$

where \mathbf{v}_{0-} is the initial velocity vector. This cost function involving absolute values can be transformed into a linear function with the introduction of new variables and inequality constraints:

$$\begin{aligned} \mathbf{v}_{0+} - \mathbf{v}_{0-} &\leq \alpha_0 \\ -(\mathbf{v}_{0+} - \mathbf{v}_{0-}) &\leq \alpha_0 \\ \mathbf{v}_{k+} - \Phi_{vr}^{[k-1]}(r_0 + \rho_{k-1}u) - \Phi_{vv}^{[k-1]}\mathbf{v}_{k-1+} &\leq \alpha_k \\ -(\mathbf{v}_{k+} - \Phi_{vr}^{[k-1]}(r_0 + \rho_{k-1}u) - \Phi_{vv}^{[k-1]}\mathbf{v}_{k-1+}) &\leq \alpha_k \\ \Delta \mathbf{v}_N &\leq \alpha_N \\ -\Delta \mathbf{v}_N &\leq \alpha_N \end{aligned} \quad (20)$$

where α_k are extra decision variables, and the cost function becomes the sum of α_k .

3.5 A semidefinite programming problem

Having defined all the different ingredients in the previous subsections, the last step consists in gathering them in a compact formulation. Therefore, a solution to the initial minimum-fuel glideslope guidance problem may be obtained via the solution of the following semidefinite programming problem:

$$\begin{aligned} \min \quad & c^T \alpha \\ \text{s.t.} \quad & (12), (13), (18) \text{ and } (20) \end{aligned}$$

with $c = [1 \dots 1]^T$ and $\alpha = [\alpha_0^T \dots \alpha_N^T]^T$. When considering a second order polynomial approximation, we have that $Y_{1il}^k \in \mathbb{R}^{4 \times 4}$, $Y_{2il}^k \in \mathbb{R}^{3 \times 3}$, $Y_{1iu}^k \in \mathbb{R}^{4 \times 4}$ and $Y_{2iu}^k \in \mathbb{R}^{3 \times 3}$.

4. NUMERICAL SIMULATION

4.1 Example 1

An illustration based on PRISMA programme (Berges et al. (2007)) is presented. In this first example, the target evolves on a quasi-circular orbit $e = 0.004$ with a semi-major axis of $a = 7011$ km. The glideslope approach is used to transfer the chaser from \mathbf{r}_0 to \mathbf{r}_T in 6 maneuvers (N) during 25 min ($T = 1500$ s),

$$\begin{aligned} X_0^T &= [r_0^T \ v_{0-}^T] = [-400 \ 40 \ -50 \ -0.5 \ 0 \ 0], \\ X_T^T &= [r_T^T \ v_T^T] = [-40 \ 0 \ -10 \ 0 \ 0 \ 0]. \end{aligned}$$

Three algorithms are compared: the classical one from Hablani et al. (2002) based on Hill-Clohesy-Wiltshire equations, its direct extension based on Yamanaka-Ankersen equations and the optimal glideslope algorithm proposed in this paper. In all cases, the resulting impulsive control sequence $\Delta \mathbf{v}_k$ is applied and propagated with the Tschauner-Hempel equations. We aim at emphasizing the significant drift induced when using the glideslope control computed with the Hill-Clohesy-Wiltshire equations even when the reference orbit is quasi-circular. Figure 3 shows the chaser trajectories for the different approaches. The final position of the chaser resulting

from the Hablani's glideslope is $[-49.2, -0.2, -16]$ m, that is 11m away from the desired position. Regarding the velocity profile along the glideslope, the relevant parameters are set such that $\dot{\rho}_0 = -1$ and $\dot{\rho}_T$ is imposed by the maneuver period T . The global consumptions of the standard circular and elliptic glideslope algorithms are quite similar and equal, respectively, 2.9705 m/s and 2.977 m/s. The specifications for the proposed algorithm are defined by a final velocity $\mathbf{v}_T = \mathbf{0}$ m/s and a constraint on the trajectory characterized by a $10 \text{ m} \times 10 \text{ m}$ corridor. The consumption obtained is 1.9698 m/s which is much lower than the standard approach. Note also that the standard trajectories do not respect the admissible corridor in green.

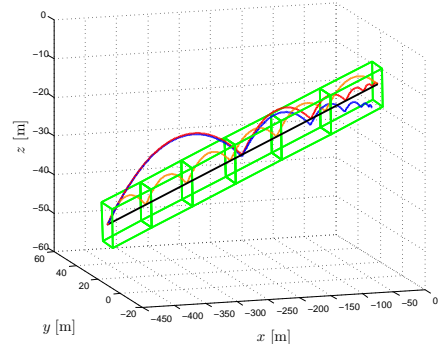


Fig. 3. Chaser relative trajectories, standard circular glideslope (blue) vs. elliptic glideslope (red) vs. proposed optimal algorithm (orange).

The sequences of impulsive maneuvers for the standard elliptic glideslope and the minimum-fuel algorithm are depicted in Figure 4 (the corresponding table with values is given in (Ariba et al., 2017)).

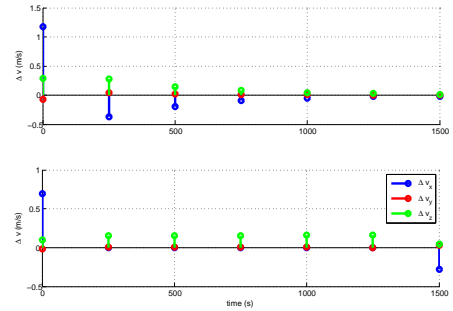


Fig. 4. Impulsive control sequences for the standard elliptic glideslope (top) and for the optimal glideslope (bottom) in example 1.

4.2 Example 2

In this second example, we present the standard elliptic glideslope approach as it may be built from the information obtained in Okasha and Newman (2011) and the proposed optimal algorithm. Those algorithms are compared in a case for which the eccentricity of the reference orbit is high. The parameters defining the conditions of the rendezvous are set as follows:

$$T = 540 \text{ s}, N = 4, n = 0.001 \text{ rad/s}, e = 0.7, \mathbf{v}_T = \mathbf{0},$$

$$\mathbf{r}_0 = \begin{bmatrix} -500 \\ 10 \\ 30 \end{bmatrix} \text{ m}, \mathbf{r}_T = \begin{bmatrix} -100 \\ 0 \\ 20 \end{bmatrix} \text{ m}, \mathbf{v}_{0-} = \begin{bmatrix} 0 \\ 0 \\ 0.5 \end{bmatrix} \text{ m/s}.$$

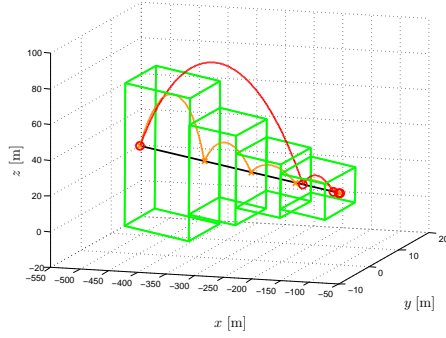


Fig. 5. Chaser relative trajectories: standard elliptic glideslope algorithm (red) vs. proposed optimal algorithm (orange).

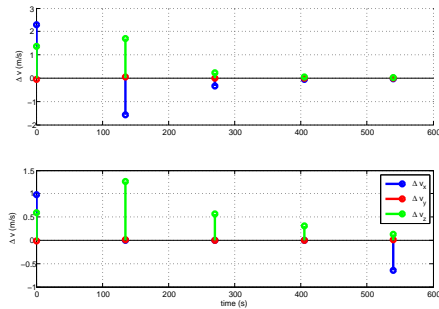


Fig. 6. Impulsive control sequences for the standard glideslope (top) and for the optimal glideslope (bottom) in example 2.

Regarding the constraints on the trajectory guidance error, we define for each maneuver a box (or a corridor) defined by 4 planes with (15). Thus, 4 boxes centered around the glideslope line are defined:

maneuver k	1	2	3	4
height δ_1 [m]	90	50	30	20
width δ_2 [m]	10	10	10	10

Figure 5 depicts the chaser trajectories for the two methods and where the four boxes corresponding to trajectory constraints are represented in green. The consumption of the standard glideslope algorithm is 7.74 m/s whereas the consumption of our optimal algorithm is 4.53 m/s . The respective sequences of impulsive maneuvers are depicted in Figure 6 (the corresponding table with values is given in (Ariba et al., 2017)).

5. CONCLUSION

In this paper, a new algorithm based on semidefinite programming has been proposed for the problem of close range impulsive glideslope rendezvous in an elliptic orbit. The two main shortcomings (regarding the lack of control on the bounds over the inherent guidance errors and the impossibility of minimizing the fuel consumption) of the classical algorithm by Hablani et al. (2002) are tackled via a combination of simple techniques mainly borrowed from the field of non negative polynomials theory. The main design feature included in the new proposed glideslope algorithm is the possibility to specify an admissible volume for each hump of the relative trajectory and therefore to control the guidance error all along the rectilinear path. Two different examples have clearly shown the key features of the exposed results like a significant improved fuel consumption with respect to

Hablani's algorithm and a user-defined bound profile on the maximum guidance error.

6. ACKNOWLEDGEMENTS

The Authors would like to thank Jean-Claude Berges from CNES and Damiana Losa from Thales Alenia Space for the grants that partly supports this activity.

REFERENCES

- Alfriend, K., Vadali, S., Gurfil, P., How, J., and Breger, L. (2010). *Spacecraft Formation Flying: Dynamics, Control and Navigation*. Astrodynamics Series. Elsevier, Burlington, MA, USA.
- Ariba, Y., Arzelier, D., and Urbina Iglesias, L.S. (2017). Optimal glideslope guidance algorithm for minimum-fuel fixed-time elliptic rendezvous. Technical report, Icam and LAAS-CNRS, Toulouse, France.
- Ariba, Y., Arzelier, D., Urbina Iglesias, L.S., and Louembet, C. (2016). V-bar and r-bar glideslope guidance algorithms for fixed-time rendezvous: a linear programming approach. In *IFAC Symposium on Automatic Control in Aerospace (ACA)*. Sherbrooke (Canada).
- Berges, J.C., Cayeux, P., Gaudel-Vacaresse, A., and Meyssignac, B. (2007). Cnes approaching guidance experiment on fiord. In *20th. International Symposium on Space Flight Dynamics*. Annapolis, Maryland, USA.
- Clohessy, W. and Wiltshire, R. (1960). Terminal guidance system for satellite rendezvous. *Journal of the Astronautical Sciences*, 27(9), 653–658.
- Deaconu, G., Louembet, C., and Théron, A. (2015). Designing continuously constrained spacecraft relative trajectories for proximity operations. *Journal of Guidance, Control, and Dynamics*, 38(7), 1208–1217.
- Fehse, W. (ed.) (2003). *Automated rendezvous and docking of spacecraft*. Cambridge Aerospace Series. Cambridge University Press, Cambridge, UK.
- Hablani, H., Tapper, M., and David J. Dana-Bashian, D. (2002). Guidance and relative navigation for autonomous rendezvous in a circular orbit. *Journal of Guidance, Control and Dynamics*, Vol. 25(No. 3).
- Lawden, D. (1963). *Optimal trajectories for space navigation*. Butterworth, London, England.
- Nesterov, Y. (2000). Squared functionals systems and optimization problems. In H. Frenck, K. Roos, T. Terlaky, and S. Zhang (eds.), *High Performance Optimization*, chapter 17, 405–440. Springer US, Boston, MA, USA.
- Okasha, M. and Newman, B. (2011). Guidance, navigation and control for satellite proximity operations using tschauner-hempel equations. In *AIAA Guidance, Navigation and Control Conference*. Portland, Oregon, USA.
- Pearson, D. (1989). The glideslope approach. *Advances in Astronautical Sciences*, 69, 109–123.
- Tschauner, J. (1967). Elliptic orbit rendezvous. *AIAA Journal*, 5(6), 1110–1113.
- Wang, F., Cao, X., and Chen, X. (2007). Guidance algorithms for the near-distance rendezvous of on-orbit-servicing spacecraft. *Transactions of Japanese Society for Aeronautical and Space Sciences*, 50(167), 9–17.
- Yamanaka, K. and Ankersen, F. (2002). New state transition matrix for relative motion on an arbitrary elliptical orbit. *Journal of Guidance, Control, and Dynamics*, 25, 60–66.